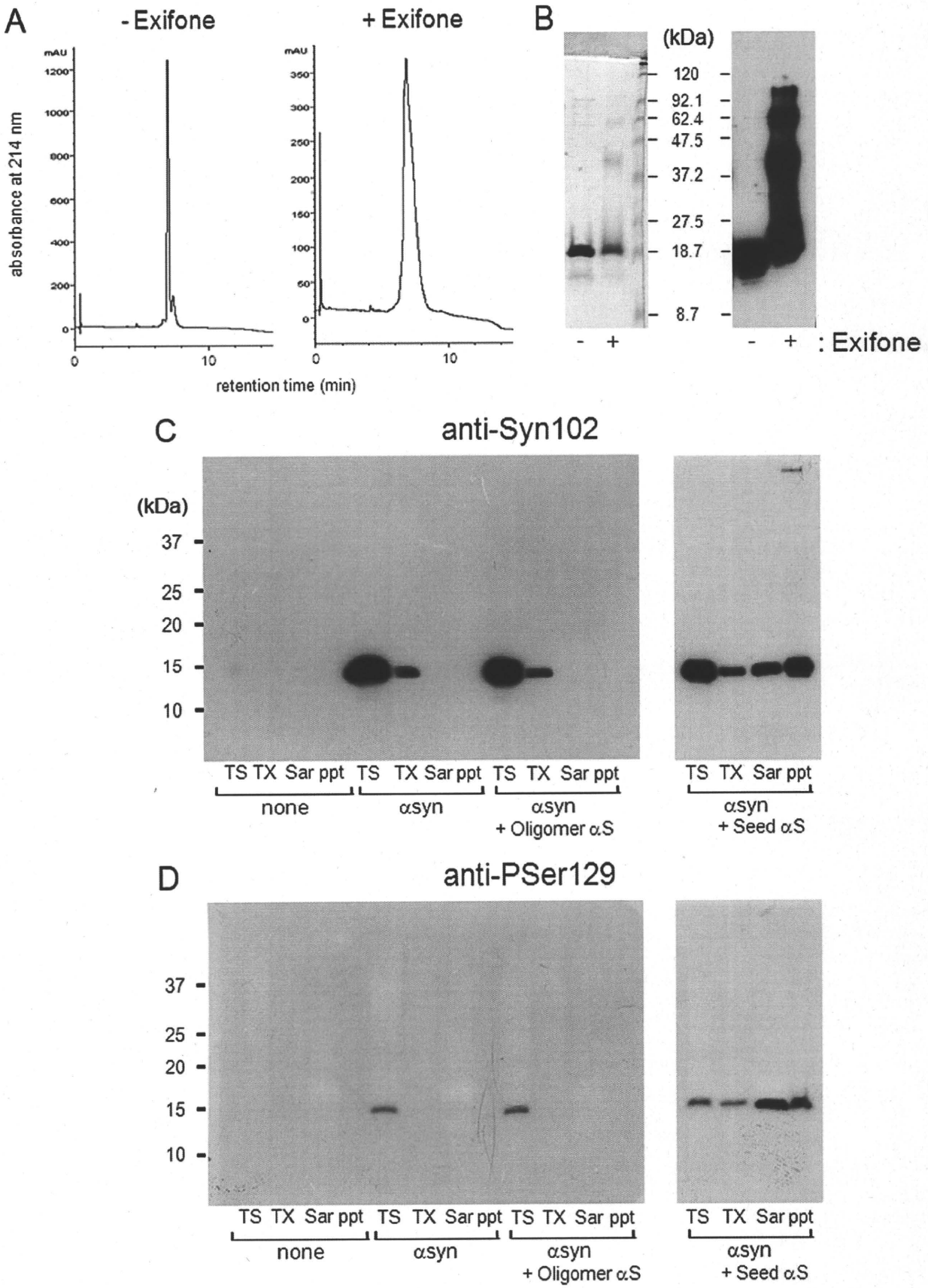

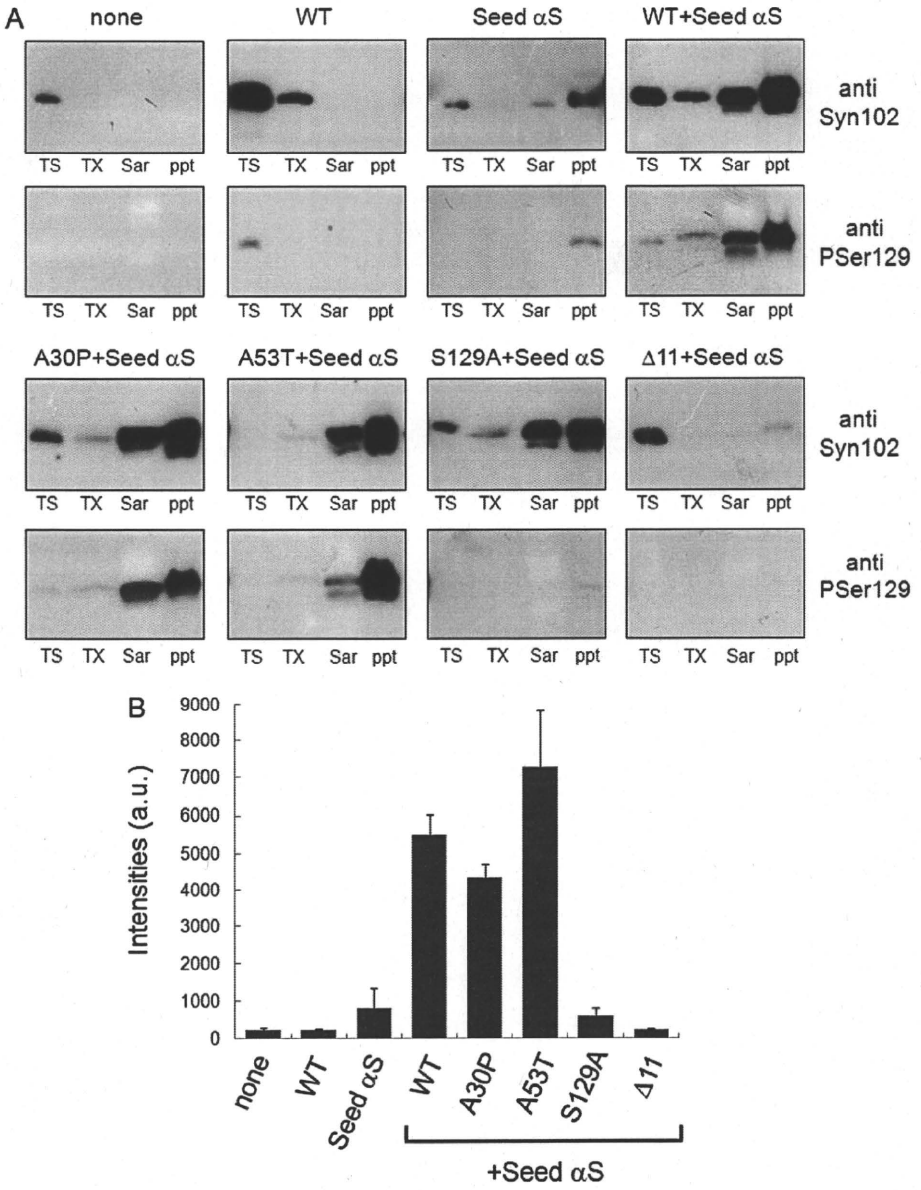

FIGURE 5. **Effects of α-syn mutations on intracellular deposition.** Immunoblot analysis of α-syn in cells transfected with pcDNA3-α-syn alone (*WT*), Seed αS alone (*Seed αS*), both WT and Seed αS (*WT + Seed αS*), and non-treated control cells (*none*). Cells overexpressing familial PD-linked A30P or A53T polymerization-deficient Δ11 mutant α-syn followed by transfection with Seed αS were also analyzed. Proteins were extracted differentially with Tris-HCl (*TS*), Triton-X (*TX*), and Sarkosyl (*Sar*), leaving the pellet (*ppt*), and immunoblotting was done with anti-Syn102 and Ser(P)^{129} (*PSer129*). The Ser(P)^{129}-immunoreactive bands detected in Sarkosyl-soluble and -insoluble fractions from each cell type shown in *A* were quantified (*B*). The results are expressed as means +S.E. (*error bars*) ($n = 3$). a.u., arbitrary unit.

revealed that the levels of Sarkosyl-insoluble α-syn in cells transfected with both α-syn and seeds were reduced by treatment with exifone or gossypetin compared with those in untreated cells (Fig. 7*B*), supporting the notion that these compounds entered the cytoplasm and blocked cell death by suppressing the seed-dependent polymerization of α-syn.

Cellular Models for Nucleation-dependent Polymerization of Tau—Beside α-syn, Tau is another major pathogenic protein that is deposited in degenerating neurons or glial cells in various neurodegenerative diseases, and aggregation of distinct Tau isoforms has been found in different diseases (*i.e.* deposition of three-repeat Tau isoforms in Pick's disease, four-repeat Tau isoforms in progressive supranuclear palsy and corticobasal degeneration, and both three- and four-repeat Tau isoforms in AD). It is unknown why distinct Tau isoforms deposit in different diseases. Thus, we also tried to establish a cellular model of intracellular Tau aggregate formation by transduction of Tau fibril seeds into cultured cells. First, we confirmed that expression of 3R1N or 4R1N by itself induced phosphorylation of Ser^{396}, but no aggregated form was detected in detergent-insoluble fractions (Fig. 8 and supplemental Fig. S5). Next, we tested whether introduced Tau 4R1N or 3R1N fibril seed (Seed 4R1N or 3R1N, respectively) is detectable by immunoblot analysis using anti-T46, anti-HT7, or anti-Ser(P)^{396} antibody. However, we could not detect any band in Triton X-100-insoluble fractions of cells treated with Seed Tau 4R1N or 3R1N in the presence of LA with any of these antibodies (data not shown). It seems likely that the efficiency of introduction of Tau 4R1N and 3R1N fibrils by LA treatment is very low, as compared with that of Seed αS. Then we checked whether treatment with recombinant Tau fibrils causes intracellular Tau aggregate formation in an LA-dependent manner. As shown in supplemental Fig. S5, LA treatment itself did not cause intracellular Tau deposition in cells expressing Tau 4R1N without

FIGURE 4. **α-Syn oligomers were not introduced into cultured cells.** *A* and *B*, α-Syn oligomers were prepared as described under "Experimental Procedures." Oligomeric α-syn protein incubated with (47.8 μg of protein) or without exifone (30 μg of protein) was analyzed by reversed-phase HPLC (Aquapore RP-300 column) (*A*). These samples (0.2 μg of protein of each) were also analyzed by SDS-PAGE and immunoblotted with anti-Syn102 (*B*). *C* and *D*, cells were transfected with empty plasmid (*none*) or pcDNA3-αsyn (*αsyn*) and then treated with or without α-syn oligomer (*Oligomer αS, 5 μg*) or fibrils (*Seed αS, 2 μg*). After incubation for 3 days, cells were harvested, and immunoblot analyses were performed. Proteins differentially extracted from the cells with Tris-HCl (*TS*), Triton X-100 (*TX*), Sarkosyl (*Sar*), and the pellet (ppt) were probed using anti-Syn102 (*C*) and anti-Ser(P)^{129} (*PSer129*) (*D*).

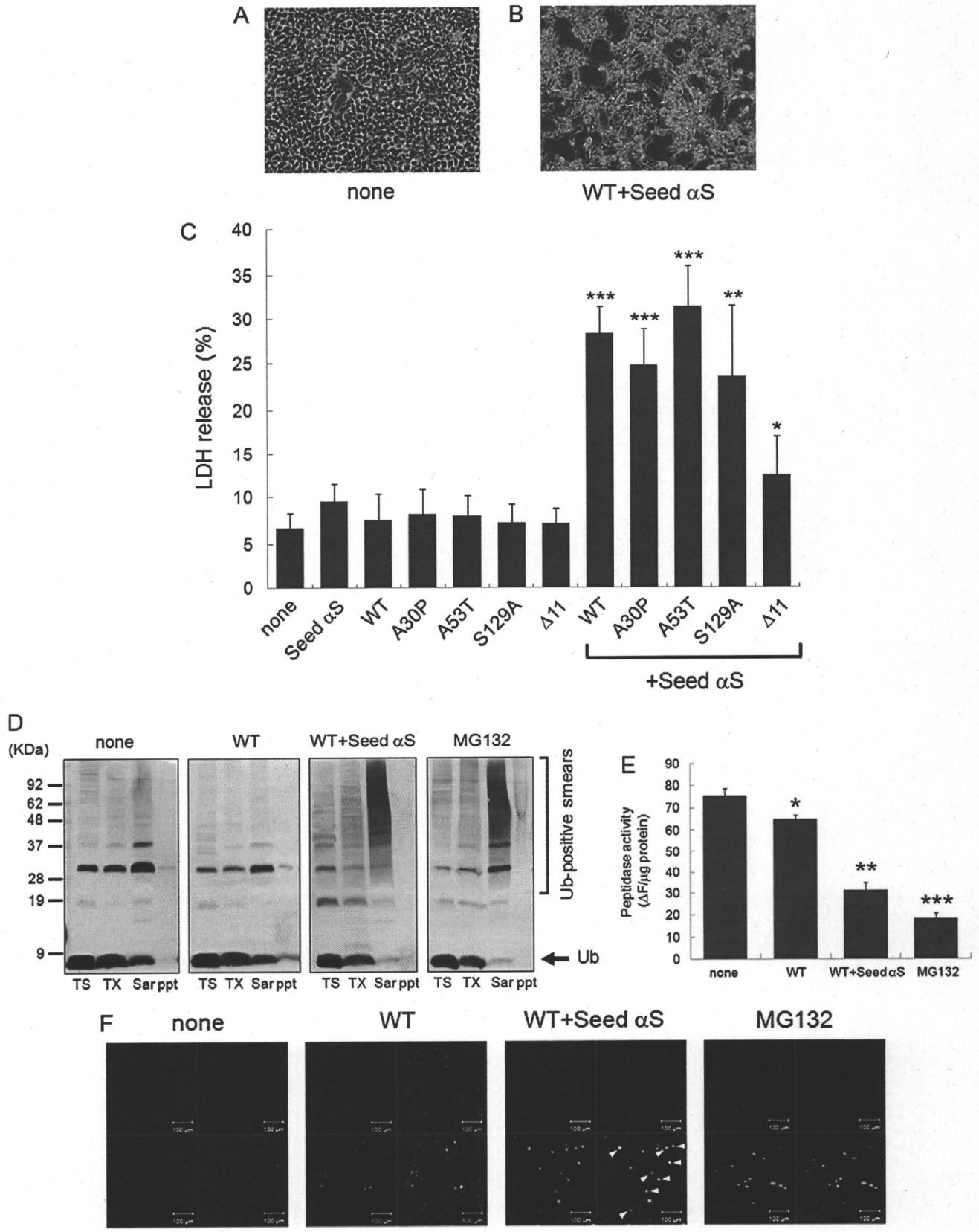

Seed 4R1N. Recombinant Tau 4R1N monomer in the presence of LA did not elicit the formation of intracellular Tau aggregates in these cells. On the other hand, when Seed 4R1N was added to cells expressing Tau 4R1N with LA, aggregated and phosphorylated Tau was detected in Sarkosyl-insoluble fractions by immunoblot analyses of these cell lysates using anti-HT7 or anti-Ser(P)^{396} antibody (supplemental Fig. S5 and Fig. 8). In the case of intracellular Tau 3R1N aggregate formation, the results were similar to those in the experiments using Tau 4R1N described above (data not shown).

Intracellular aggregated four- or three-repeat Tau was also found to be detected with not only anti-Ser(P)^{396} but also anti-AT100 antibody in the Sarkosyl-insoluble fraction (Fig. 8, *B* and *C*). Phosphorylated and deposited Tau was not found in the Triton X-100-insoluble fraction of Tau-expressing cells without Tau seed treatment or mock plasmid-expressing cells treated with Tau seed. In accordance with findings described earlier in this paper, these results suggested that soluble four- or three-repeat Tau expressed from the plasmid was accumulated into intracellular inclusions in the presence of small amounts of Seed 4R1N or 3R1N.

We also found that hyperphosphorylated and aggregated Tau was not detected in three-repeat Tau-expressing cells treated with Seed 4R1N (Fig. 8, *B* and *C*). On the other hand, the aggregated form of three-repeat Tau was detected in Triton X-100-insoluble fractions of three-repeat Tau-expressing cells treated with Seed 3R1N, and hyperphosphorylation at Ser^{396} and Ser^{212}/Thr^{214} was observed in fractionated samples of these cells, whereas no such bands were detected in four-repeat Tau-expressing cells treated with Seed 3R1N (Fig. 8, *B* and *C*). These results clearly showed that four-repeat Tau fibrils can be seeds for polymerization of four-repeat Tau, and three-repeat Tau fibrils can be seeds for polymerization of three-repeat Tau. Tau does not polymerize (cross-seed) in the presence of seeds of a different isoform. Similarly, no Tau aggregation was detected in Tau-expressing cells treated with α-syn fibril seeds (supplemental Fig. S3, *C* and *D*), and no α-syn aggregation was detected in α-syn-expressing cells transduced with Tau fibril seeds (data not shown). Furthermore, we observed anti-AT100 and anti-Ser(P)^{396}-positive Tau 4R1N or 3R1N filaments of ~15-nm width by negative stain electron microscopic analyses of Sarkosyl-insoluble fractions of cells transfected with both Tau plasmid and the seeds (Fig. 9, *A–D*).

Confocal microscopic analyses also showed that GFP-tagged Tau 4R1N (GFP-Tau 4R1N) is aggregated into round inclusions in the presence of Seed 4R1N together with LA (Fig. 8*E*). No inclusion-like structures were found in cells expressing GFP-Tau 4R1N (Fig. 8*D*) or in cells expressing GFP-Tau 4R1N after treatment with Seed 3R1N (data not shown). The ratio of the round aggregates to all GFP-positive transfectants was calculated to be 5.8% ± 0.8602 ($p = 0.0002$ by Student's *t* test against the value of cells expressing GFP-4R1N, $n = 5$). Significant cell death was not observed in cells containing intracellular 3R1N or 4R1N aggregates (data not shown). These results strongly suggest that proteins assemble easily into amyloid fibrils in the presence of amyloid seeds derived from the same protein but not a different protein.

DISCUSSION

Nucleation-dependent protein polymerization occurs in many well characterized physiological processes (*e.g.* microtubule assembly and actin polymerization). It is also the mechanism of amyloid fibril formation in various pathological conditions and has been confirmed to occur *in vitro* for a wide variety of extracellular amyloids, such as Aβ peptides and prion proteins (12, 13) as well as intracellular proteins, such as α-syn and Tau (29, 30, 42). Both extra- and intracellular amyloids have been well studied *in vitro*, but much less is known about the mechanisms of assembly *in vivo*. Here we report a simple and effective method to introduce polymerization seeds into cells using Lipofectamine, a widely used transfection reagent. This method enabled us to evaluate the nucleation-dependent polymerization of α-synuclein and to establish a cellular model of the neurodegeneration seen in Parkinson disease.

Lipofectamine is a reagent widely used for the transfection of DNA into eukaryotic cells through the formation of liposomes of polycationic and neutral lipids in water, based on the principle of cell fusion. Various methods, including microinjection, the calcium phosphate method, the DEAE-dextran method, electroporation, and viral transfer, have been employed to introduce substances that are not normally incorporated into eukaryotic cells under physiological conditions. Microinjection is versatile but is not efficient in experiments involving large numbers of cells, and the traumatic damage to cells hampers evaluation of cytotoxic effects. Here, we have successfully employed lipofection to introduce protein aggregates as seeds

FIGURE 6. **Cell death caused by formation of intracellular α-syn inclusions.** *A* and *B*, phase-contrast microscopy of the control cells (*A*) and cells transfected with both pcDNA3-α-syn and Seed αS (*B*) 3 days after treatment with Seed αS (20× objective). *C*, the extent of cell death of transfected cells was quantified using an LDH release assay. Cells transfected with α-syn plasmid alone (WT, A30P, A53T, S129A, or Δ11) or with both wild-type or several mutants and Seed αS were incubated, and the cell death assay was performed 3 days thereafter. The results are expressed as means +S.E. (*error bars*) ($n = 5$). *, not significant; **, $p < 0.01$; ***, $p < 0.0005$ by Student's *t* test against the value of Seed αS. *D–F*, impairment of proteasome activity caused by intracellular aggregates of α-syn. *D*, immunoblot analysis of proteins sequentially extracted from non-treated cells (*none*) and cells transfected with wild-type α-syn plasmid alone (*WT*) or with both pcDNA3-α-syn and Seed αS (*WT + Seed αS*) and cells treated with 1 μM MG132 for 16 h (MG132) using anti-ubiquitin antibody. An *arrow* indicates monomeric ubiquitin. Polyubiquitinated proteins, reflecting impairment of the proteasome activity, are observed in the Sarkosyl-soluble fraction. *TS*, Tris-soluble; *TX*, 1% Triton X-100-soluble; *Sar*, 1% Sarkosyl-soluble; *ppt*, Sarkosyl-insoluble and SDS-soluble. *E*, peptide hydrolysis activity of proteasome. Cytosol fractions of non-treated control cells (*none*), cells transfected with wild-type α-syn plasmid alone (*WT*) or with WT and Seed αS (*WT + Seed αS*), and cells treated with 20 μM MG132 for 4 h (*MG132*) were prepared and assayed using benzyloxycarbonyl-Leu-Leu-Glu-7-amido-4-methylcoumarin as a substrate. The results are expressed as means +S.E. ($n = 3$). *, $p < 0.05$; **, $p < 0.01$; ***, $p < 0.0005$ by Student's *t* test against the value of none. *F*, proteasome activity in cells having intracellular aggregates of α-syn. SH-SY5Y cells transfected with both GFP-CL1 and WT were treated with Seed αS for 2 days, fixed, and stained with anti-Ser(P)^{129}. In the staining of cells transfected with wild-type α-syn plasmid alone (*WT*), anti-Syn102 was used. As a control, untreated or MG132-treated cells were also stained and analyzed. In untreated control cells, the fluorescence of GFP was poorly detected because GFP-CL1 could be degraded by proteasome in cells. In cells treated with MG132, fluorescence was markedly increased as compared with that in untreated cells because of the inhibition of proteasome activity by MG132. Co-localized images (*arrowheads*) with both increased intensities of GFP (*green*) and the fluorescence of anti-Ser(P)^{129} (*red*) were detected in cells transfected with both WT and Seed αS (*WT + Seed αS*), indicating that the proteasome activity in these cells was inhibited.

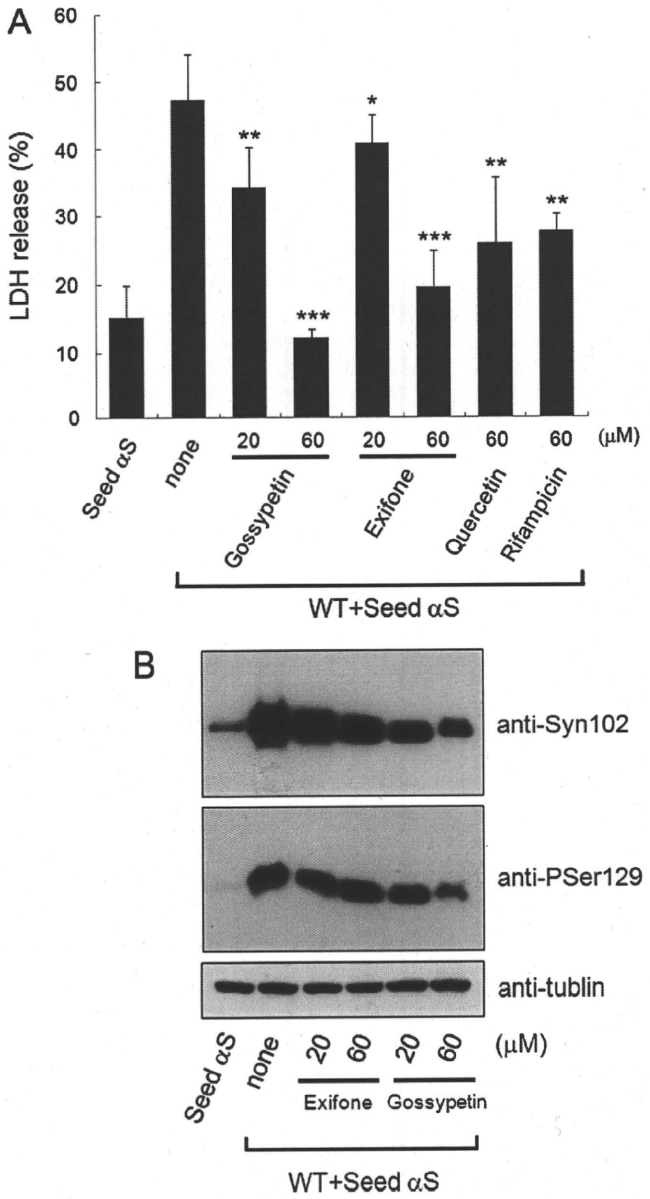

FIGURE 7. **Small molecular inhibitors of amyloid filament formation protect against cell death caused by intracellular α-syn aggregates.** *A*, the cell death of cells transfected with Seed αS and with both α-syn plasmid (*WT*) and Seed αS in the presence or absence of 20 or 60 μM gossypetin, 20 or 60 μM exifone, 60 μM quercetin, or 60 μM rifampicin was quantified by LDH release assay. The results are expressed as means ± S.E. (*error bars*) ($n = 4$). *, not significant; **, $p < 0.05$; ***, $p < 0.0005$ by Student's *t* test against the value of none. *B*, immunoblot analyses of the Sarkosyl-insoluble fraction prepared from cells transfected with Seed αS and with both WT and Seed αS in the absence or presence of exifone or gossypetin, with anti-Syn102 and anti-Ser(P)^{129} (*PSer129*) antibodies. Doubly transfected cells were treated with 20 or 60 μM exifone or gossypetin 2 h after transfection of Seed αS and cultured for 3 days in the presence of polyphenols. Tubulin-α loading controls are also shown.

for amyloid fibril formation (patent pending for the United States (12/086124), the European Union (06834541.2), and Japan (2007-549210)). The reason why Lipofectamine could specifically incorporate Seed αS but not soluble α-syn into cells is unknown. However, one possibility is that aggregated α-syn with an ordered filamentous structure was preferentially bound to Lipofectamine and formed a complex that could be more effectively transported into cells compared with soluble α-syn, which has a random coil structure. In line with this idea, it has been reported that yeast prion fibrils can be introduced into yeast cells (31). Recently, Luk *et al.* (32) have also reported that α-syn monomers and fibrils but not oligomers were introduced into cells by Bioporter, a cationic-liposomal protein transduction reagent.

We confirmed the incorporation of insoluble α-syn seeds into cells by detecting phosphorylation of α-syn, as has been seen in intracellular aggregates of α-syn in various neurodegenerative conditions referred to as synucleinopathies. This suggests that Seed αS introduced into cells is a good target for phosphorylation at Ser^{129}. In contrast to our results, a recent report suggested that α-syn fibrils were not phosphorylated after internalization (32). It is possible that this specific phosphorylation represents an active attempt by cells to maintain the intracellular milieu by sequestering protein species that are harmful to cells. Notably, the phosphorylation of α-syn was dramatically increased when Seed αS was introduced into cells overexpressing soluble α-syn (Fig. 3 and supplemental Figs. S1*D* and S2). The possibility therefore arises that widespread propagation of hyperphosphorylation of α-syn throughout the cytoplasm reflects the activation of a certain kinase(s) associated with conversion of soluble α-syn into the fibrillar form in the presence of Seed αS. However, further investigation is needed to elucidate the importance of phosphorylation for protein aggregation.

The significance of intracellular and extracellular protein aggregates in neurodegeneration is still a matter of debate. The present results clearly show that nucleation-dependent polymerization of amyloid-like proteins is closely related to neuronal degeneration leading to cell death. According to the seeding theory, amyloid fibrils grow rapidly, without a time lag, when seeds are exposed to an amount of amyloidogenic soluble protein that exceeds the critical concentration. Our experiments with seed-transfected SH-SY5Y cells overexpressing α-syn clearly demonstrated that this is the case in the intracellular environment. We have unequivocally demonstrated that nucleation-dependent polymerization of amyloid-like fibrils can occur inside cells, and the intracellular filament formation elicits a variety of cellular reactions, including hyperphosphorylation and compromise of the ubiquitin proteasome system. We also showed that α-syn oligomers were not introduced into cells by LA and did not function as seeds for α-syn aggregate formation in cultured cells. It has been speculated that protein fibrils, not oligomers, are spread or transmitted in recently reported *in vivo* models (25, 33).

Our study also revealed that intracellular protein aggregation is highly dependent on the species of protein fibril seeds. This important finding may explain why only certain Tau isoforms are deposited in several tauopathies, including Pick disease, progressive supranuclear palsy, and corticobasal degeneration. In this study, α-syn fibrils were shown to be unable to seed intracellular Tau aggregation, which is consistent with neuropathological reports that deposited α-syn is not markedly colocalized with Tau aggregates. Our observations strongly support a seed-dependent mechanism for the formation of the intracellular protein aggregates.

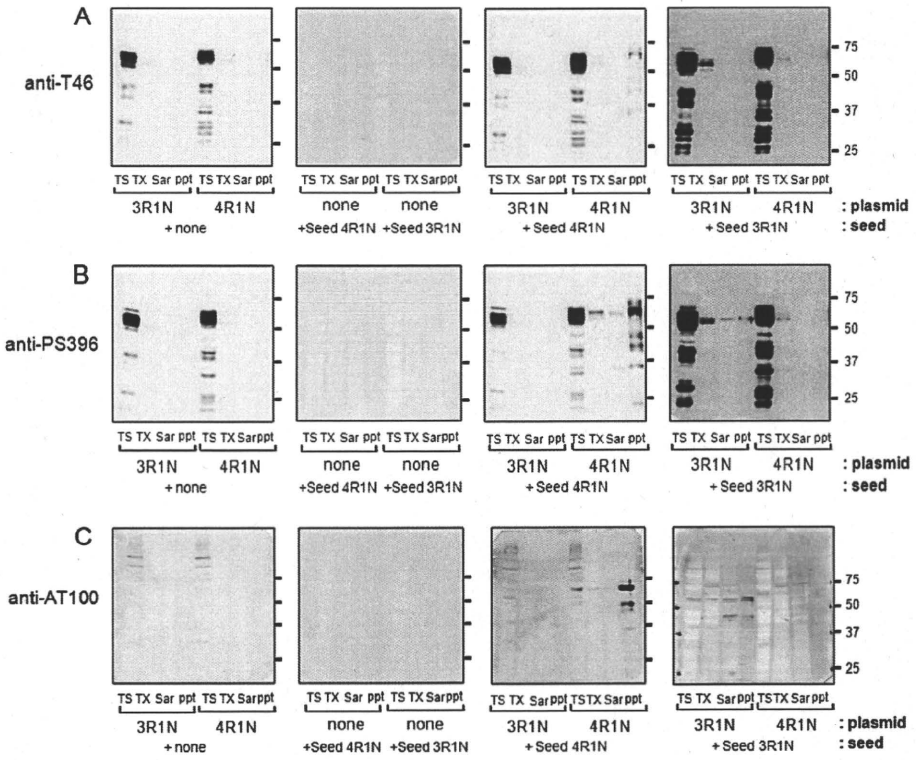

FIGURE 8. **Immunoblot analyses of intracellular Tau aggregates.** *A–C*, immunoblot analysis of Tau in cells treated with Tau fibrils alone (Seed 3R1N or Seed 4R1N), pcDNA3-Tau alone (3R1N or 4R1N), or both Seed Tau and pcDNA3-Tau. Tau proteins differentially extracted from the cells with Tris-HCl (*TS*), Triton X-100 (*TX*) and Sarkosyl (*Sar*), and the pellet (*ppt*) were probed with anti-T46 (*A*), anti-Ser(P)^{396} (*PS396*) (*B*), and anti-AT100 (*C*).

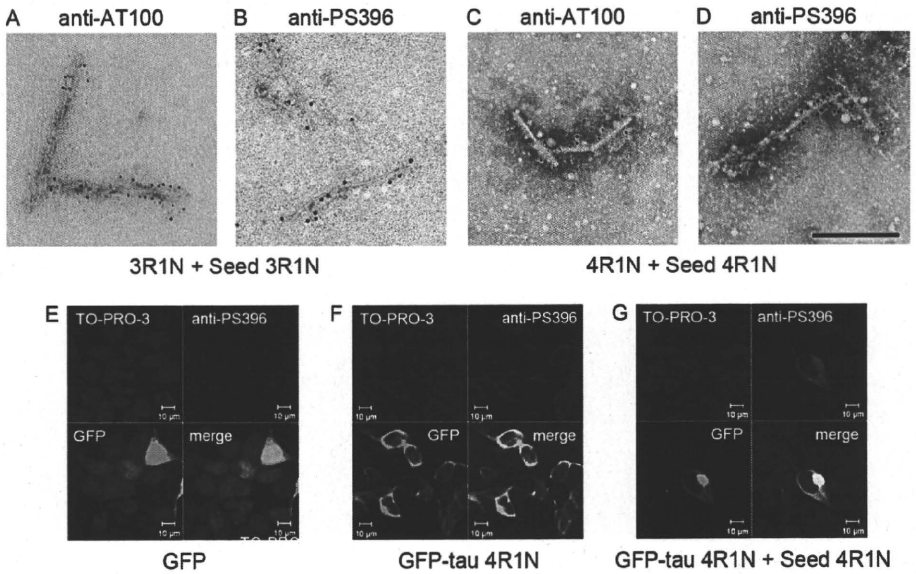

FIGURE 9. **Cellular models for intracellular Tau aggregation.** *A–D*, immunoelectron microscopy of Tau filaments extracted from transfected cells. SH-SY5Y cells were transfected with both pcDNA3-Tau 3R1N and Seed 3R1N (*A* and *B*) or pcDNA3-Tau 4R1N and Seed 4R1N (*C* and *D*). The Sarkosyl-insoluble fraction was prepared from the cells, and the filaments were immunolabeled with anti-AT100 (*A* and *C*) or anti-Ser(P)^{396} (*PS396*) (*B* and *D*) antibody. *Scale bar*, 200 nm. *E–G*, confocal laser microscopic analyses of SH-SY5Y cells transfected with pEGFP empty vector (*E*), pEGFP-Tau 4R1N (*F*), and cells transfected with both pEGFP-Tau 4R1N and Seed 4R1N (*G*), immunostained with anti-Ser(P)^{396} (*red*), and counterstained with TO-PRO-3 (*blue*). *Scale bars*, 10 μm.

shed from one cell may easily be propagated to others (*e.g.* neurons or glial cells) under pathological conditions (*e.g.* alteration in membrane permeability due to aging or virus infection, impairment of membrane function as a result of physical interaction with extracellular amyloid deposits, or abnormal membrane depolarization) that favor intracellular deposition of protein fibrils.

It remains to be clarified whether the incorporation of amyloid seeds into neurons or glial cells, as shown in this study, also occurs *in vivo*. However, some observations in AD or in transgenic animals support this possibility; apolipoprotein E (apoE) is involved in lipoprotein particle uptake mediated by cell surface receptors, and the E4 allele is the strongest genetic risk factor for AD. The apoE polypeptide has also been shown to bind Aβ (34), Tau (35), and the non-Aβ component of Alzheimer disease region of α-syn (36) and to be localized in amyloid plaques and neurofibrillary tangles in AD and prion plaques (37) in Creutzfeldt-Jakob disease. ApoE and low density lipoprotein receptor-related protein facilitate intraneuronal Aβ42 accumulation in transgenic mice (38). Furthermore, activation of both endocytic uptake and recycling of these proteins at a preclinical stage has been reported in sporadic AD and Down syndrome (39). Thus, it is strongly suggested that extracellular amyloid may be taken up into neurons by apoE and lipoprotein receptor-related protein-mediated endocytosis. Therefore, intracellular amyloid seeds composed of α-syn or Tau may also be incorporated into neurons by similar mechanisms when these seeds are released to the extracellular space after neuronal death.

It is well established that Tau protein starts to accumulate in the entorhinal region and spreads to the neocortices, closely correlating with the progression of AD (40). Similarly, accumulation of phosphorylated α-syn has been shown to start in vulnerable regions (*i.e.* limbic cortices) and to spread to the neocortices in PD or DLB. However, the mechanism of propagation of abnormal

Importantly, we showed that seed α-syn or Tau, an insoluble aggregate prepared from α-syn or Tau filaments, is effectively incorporated into cells by lipofection. This, in turn, suggests that high molecular weight protein aggregates or amyloid seeds

protein deposition remains unknown. This study strongly supports a seed-dependent mechanism for the formation of the intracellular protein aggregates. In the context of our propagation hypothesis, it will be crucial to inhibit not only the production of intracellular amyloid seeds but also their spread into the extracellular space. Vaccination against the intracellular amyloid proteins, such as α-syn (41) or Tau may be an effective approach, together with inhibition of intracellular amyloid filament formation by small molecular inhibitors, for the therapy of these diseases.

Acknowledgments—We thank Yoko Shimomura, Masami Masuda, and Ayaho Dan for technical assistance with immunoelectron microscopy and the preparation of recombinant Tau protein. We also thank Michel Goedert for helpful comments on the manuscript.

REFERENCES

1. Chiti, F., and Dobson, C. M. (2006) *Annu. Rev. Biochem.* **75,** 333–366
2. Goedert, M., Spillantini, M. G., and Davies, S. W. (1998) *Curr. Opin Neurobiol.* **8,** 619–632
3. Prusiner, S. B. (2001) *N. Engl. J. Med.* **344,** 1516–1526
4. Soto, C., Estrada, L., and Castilla, J. (2006) *Trends Biochem. Sci.* **31,** 150–155
5. Fujiwara, H., Hasegawa, M., Dohmae, N., Kawashima, A., Masliah, E., Goldberg, M. S., Shen, J., Takio, K., and Iwatsubo, T. (2002) *Nat. Cell Biol.* **4,** 160–164
6. Kirschner, D. A., Inouye, H., Duffy, L. K., Sinclair, A., Lind, M., and Selkoe, D. J. (1987) *Proc. Natl. Acad. Sci. U.S.A.* **84,** 6953–6957
7. Eanes, E. D., and Glenner, G. G. (1968) *J. Histochem. Cytochem.* **16,** 673–677
8. Nguyen, J. T., Inouye, H., Baldwin, M. A., Fletterick, R. J., Cohen, F. E., Prusiner, S. B., and Kirschner, D. A. (1995) *J. Mol. Biol.* **252,** 412–422
9. Serpell, L. C., Berriman, J., Jakes, R., Goedert, M., and Crowther, R. A. (2000) *Proc. Natl. Acad. Sci. U.S.A.* **97,** 4897–4902
10. Berriman, J., Serpell, L. C., Oberg, K. A., Fink, A. L., Goedert, M., and Crowther, R. A. (2003) *Proc. Natl. Acad. Sci. U.S.A.* **100,** 9034–9038
11. Perutz, M. F. (1999) *Trends Biochem. Sci.* **24,** 58–63
12. Harper, J. D., and Lansbury, P. T., Jr. (1997) *Annu. Rev. Biochem.* **66,** 385–407
13. Jarrett, J. T., and Lansbury, P. T., Jr. (1993) *Cell* **73,** 1055–1058
14. Jakes, R., Spillantini, M. G., and Goedert, M. (1994) *FEBS Lett.* **345,** 27–32
15. Nonaka, T., Iwatsubo, T., and Hasegawa, M. (2005) *Biochemistry* **44,** 361–368
16. Aoyagi, H., Hasegawa, M., and Tamaoka, A. (2007) *J. Biol. Chem.* **282,** 20309–20318
17. Taniguchi, S., Suzuki, N., Masuda, M., Hisanaga, S., Iwatsubo, T., Goedert, M., and Hasegawa, M. (2005) *J. Biol. Chem.* **280,** 7614–7623
18. Nonaka, T., Kametani, F., Arai, T., Akiyama, H., and Hasegawa, M. (2009) *Hum. Mol. Genet.* **18,** 3353–3364
19. Nonaka, T., and Hasegawa, M. (2009) *Biochemistry* **48,** 8014–8022
20. Sung, J. Y., Kim, J., Paik, S. R., Park, J. H., Ahn, Y. S., and Chung, K. C. (2001) *J. Biol. Chem.* **276,** 27441–27448
21. Spillantini, M. G., Crowther, R. A., Jakes, R., Hasegawa, M., and Goedert, M. (1998) *Proc. Natl. Acad. Sci. U.S.A.* **95,** 6469–6473
22. Conway, K. A., Rochet, J. C., Bieganski, R. M., and Lansbury, P. T., Jr. (2001) *Science* **294,** 1346–1349
23. Masuda, M., Suzuki, N., Taniguchi, S., Oikawa, T., Nonaka, T., Iwatsubo, T., Hisanaga, S., Goedert, M., and Hasegawa, M. (2006) *Biochemistry* **45,** 6085–6094
24. Giasson, B. I., Murray, I. V., Trojanowski, J. Q., and Lee, V. M. (2001) *J. Biol. Chem.* **276,** 2380–2386
25. Desplats, P., Lee, H. J., Bae, E. J., Patrick, C., Rockenstein, E., Crews, L., Spencer, B., Masliah, E., and Lee, S. J. (2009) *Proc. Natl. Acad. Sci. U.S.A.* **106,** 13010–13015
26. Hasegawa, M., Fujiwara, H., Nonaka, T., Wakabayashi, K., Takahashi, H., Lee, V. M., Trojanowski, J. Q., Mann, D., and Iwatsubo, T. (2002) *J. Biol. Chem.* **277,** 49071–49076
27. Bence, N. F., Sampat, R. M., and Kopito, R. R. (2001) *Science* **292,** 1552–1555
28. Gilon, T., Chomsky, O., and Kulka, R. G. (1998) *EMBO J.* **17,** 2759–2766
29. Friedhoff, P., von Bergen, M., Mandelkow, E. M., Davies, P., and Mandelkow, E. (1998) *Proc. Natl. Acad. Sci. U.S.A.* **95,** 15712–15717
30. Wood, S. J., Wypych, J., Steavenson, S., Louis, J. C., Citron, M., and Biere, A. L. (1999) *J. Biol. Chem.* **274,** 19509–19512
31. Tanaka, M., Chien, P., Yonekura, K., and Weissman, J. S. (2005) *Cell* **121,** 49–62
32. Luk, K. C., Song, C., O'Brien, P., Stieber, A., Branch, J. R., Brunden, K. R., Trojanowski, J. Q., and Lee, V. M. (2009) *Proc. Natl. Acad. Sci. U.S.A.* **106,** 20051–20056
33. Clavaguera, F., Bolmont, T., Crowther, R. A., Abramowski, D., Frank, S., Probst, A., Fraser, G., Stalder, A. K., Beibel, M., Staufenbiel, M., Jucker, M., Goedert, M., and Tolnay, M. (2009) *Nat. Cell Biol.* **11,** 909–913
34. Strittmatter, W. J., Saunders, A. M., Schmechel, D., Pericak-Vance, M., Enghild, J., Salvesen, G. S., and Roses, A. D. (1993) *Proc. Natl. Acad. Sci. U.S.A.* **90,** 1977–1981
35. Strittmatter, W. J., Saunders, A. M., Goedert, M., Weisgraber, K. H., Dong, L. M., Jakes, R., Huang, D. Y., Pericak-Vance, M., Schmechel, D., and Roses, A. D. (1994) *Proc. Natl. Acad. Sci. U.S.A.* **91,** 11183–11186
36. Olesen, O. F., Mikkelsen, J. D., Gerdes, C., and Jensen, P. H. (1997) *Brain Res. Mol. Brain Res.* **44,** 105–112
37. Namba, Y., Tomonaga, M., Kawasaki, H., Otomo, E., and Ikeda, K. (1991) *Brain Res.* **541,** 163–166
38. Zerbinatti, C. V., Wahrle, S. E., Kim, H., Cam, J. A., Bales, K., Paul, S. M., Holtzman, D. M., and Bu, G. (2006) *J. Biol. Chem.* **281,** 36180–36186
39. Cataldo, A. M., Peterhoff, C. M., Troncoso, J. C., Gomez-Isla, T., Hyman, B. T., and Nixon, R. A. (2000) *Am. J. Pathol.* **157,** 277–286
40. Braak, H., and Braak, E. (1991) *Acta Neuropathol.* **82,** 239–259
41. Masliah, E., Rockenstein, E., Adame, A., Alford, M., Crews, L., Hashimoto, M., Seubert, P., Lee, M., Goldstein, J., Chilcote, T., Games, D., and Schenk, D. (2005) *Neuron* **46,** 857–868
42. Yonetani, M., Nonaka, T., Masuda, M., Inukai, Y., Oikawa, T., Hisanaga, S. I., and Hasegawa, M. (2009) *J. Biol. Chem.* **284,** 7940–7950

Supplemental data

Seeded aggregation and toxicity of α-synuclein and tau: cellular models of neurodegenerative diseases

Takashi Nonaka, Sayuri T. Watanabe, Takeshi Iwatsubo, Masato Hasegawa

Supplemental figure legends

Figure S1. Time-course observation of cells transduced with Seed αS.
(A-B) Electron microscopic analyses of Seed αS used in this study with (B) or without (A) sonication before use. Scale bars, 200 nm.
(C) Confocal microscopic images of SH-SY5Y cells 1 day and 3 days after treatment with Seed-HA in the presence or absence of LA. Cells were stained with anti-HA (red), anti-PSer129 (green) and TO-PRO-3 (blue). Scale bars, 50 μm.
(D) Confocal microscopic images of SH-SY5Y cells transfected with or without pcDNA3-αsyn (WT) 1 day and 3 days after treatment with or without Seed-HA. Cells were stained with anti-HA (red), anti-PSer129 (green) and TO-PRO-3 (blue). Scale bars, 50 μm.

Figure S2. Intracellular α-syn aggregate formation is dependent on the amount of α-syn seeds.
Cells were transfected with pcDNA3-αsyn (αsyn) and then transduced with different amounts of Seed-HA. After incubation for 3 days, cells were harvested and immunoblot analyses of the lysates was performed. α-Syn differentially extracted from the cells with Tris-HCl (TS), Triton X-100 (TX), and Sarkosyl (Sar), and the pellet (ppt), were probed using anti-HA (A) and anti-PSer129 (B). Immunoreactivity of phosphorylated α-syn in the TX-insoluble fraction was quantified using anti-PSer129. The results are shown in (C).

Figure S3. α-Syn fibrils seed intracellular aggregate formation of plasmid-derived α-syn, but not tau.
Cells were transfected with empty plasmid (none), pcDNA3-αsyn (αsyn) or pcDNA3-tau 3R1N (3R1N) and then treated with Seed-HA. After incubation for 3 days, cells were harvested and immunoblot analyses were performed. Proteins differentially extracted from the cells with Tris-HCl (TS), Triton X-100 (TX), and Sarkosyl (Sar), and the pellet (ppt), were probed using

anti-HA (A), anti-PSer129 (B), anti-T46 (C) and anti-PS396 (D).

Figure S4. Apoptosis is not induced in cells harboring intracellular α-syn aggregates.
(A) TUNEL staining of cells treated without (none) or with 1 μM staurosporine (stsp) for 8 hr and cells transfected with or without pcDNA3-αsyn (WT) 3 days after treatment with or without Seed αS. Cells were stained with TUNEL reagent (green), anti-PSer129 (red) and TO-PRO-3 (blue). Scale bars, 100 μm.
(B) The measurement of caspase-3 activity in cultured cells. Cells were transfected with empty plasmid (none) or pcDNA3-αsyn (WT) and then treated with or without Seed αS. After incubation for 3 days, cells were harvested and caspase-3 activity in the lysates was measured using Ac-DEVD-MCA as a substrate. Cell lysate treated with stsp was used as a positive control.

Fig. S5. Introduction of tau 4R1N monomer and fibril seed by Lipofectamine.

Purified recombinant tau (4R1N monomer; 2 μg) and filaments (Seed 4R1N, 2 μg) were sonicated and then incubated with Lipofectamine (LA). The protein-LA complexes were dispersed in opti-MEM and added to SH-SY5Y cells expressing pcDNA3-tau 4R1N. After 48 hr of culture, the cells were collected in the presence of 0.25% trypsin, and tau proteins were differentially extracted from the cells with Tris-HCl (TS), Triton X-100 (TX) and Sarkosyl (Sar), and the pellet (ppt), were probed with anti-T46 (upper), anti-HT7 (middle) and anti-PS396 (lower).

Fig. S1 Nonaka et al

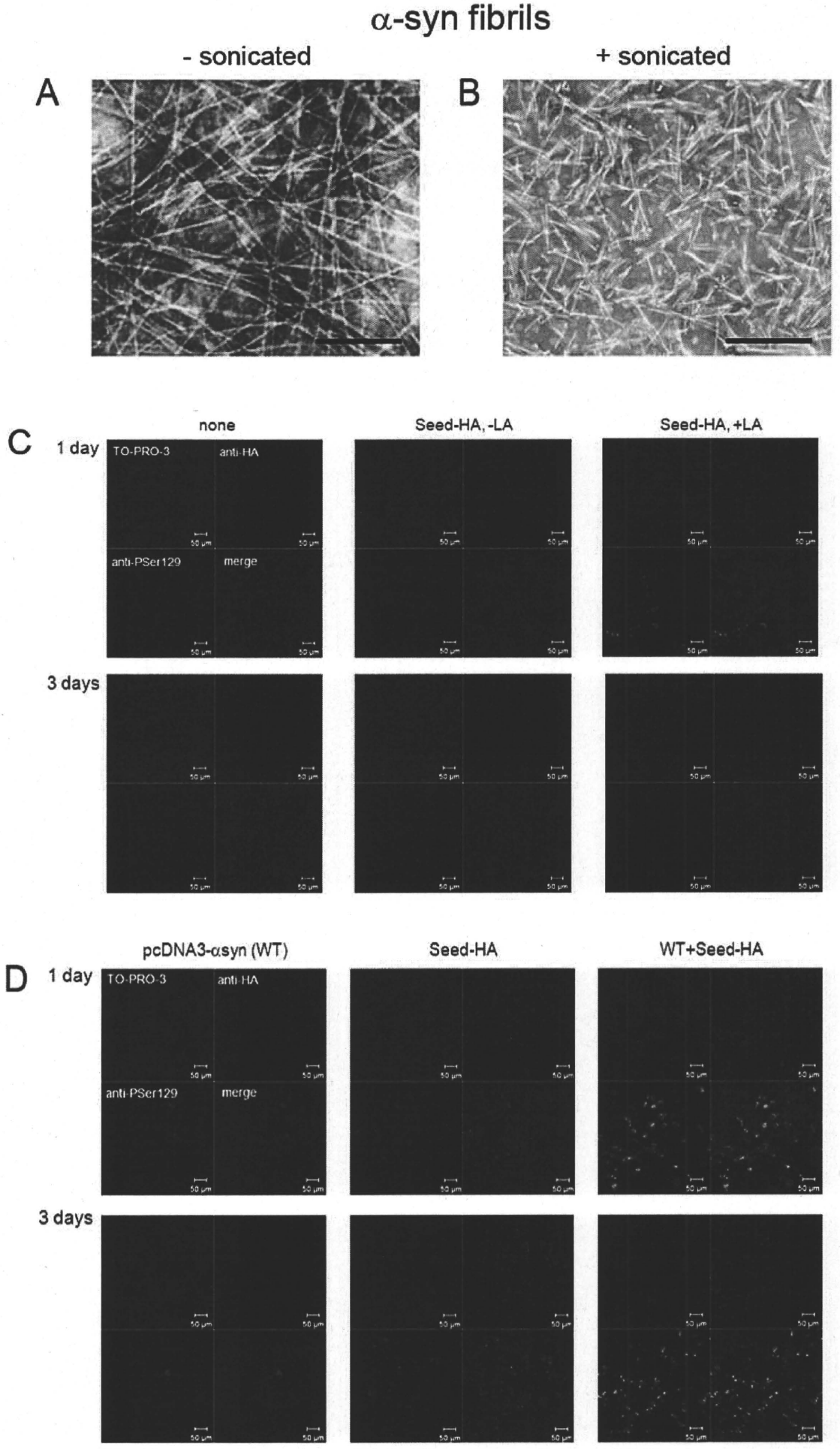

Fig. S2 Nonaka et al

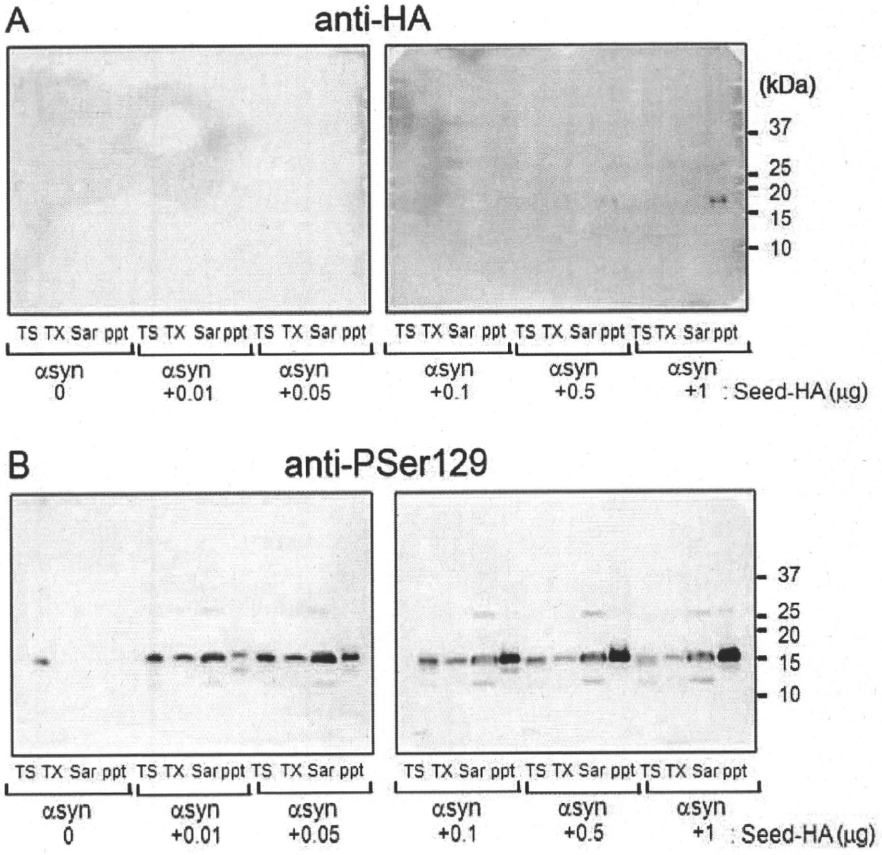

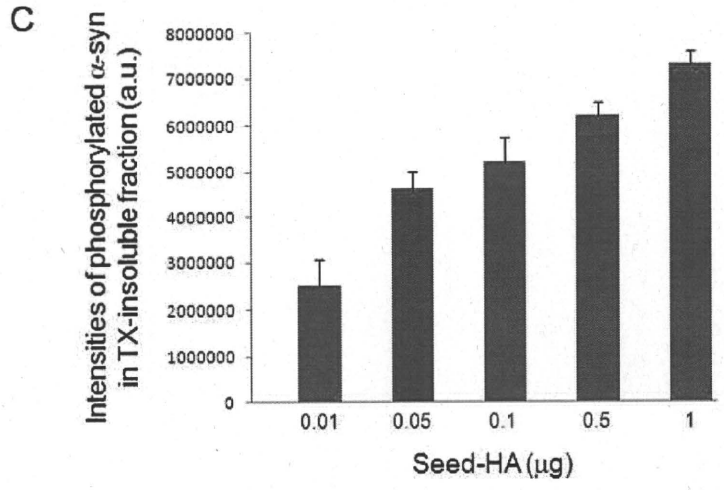

Fig. S3 Nonaka et al

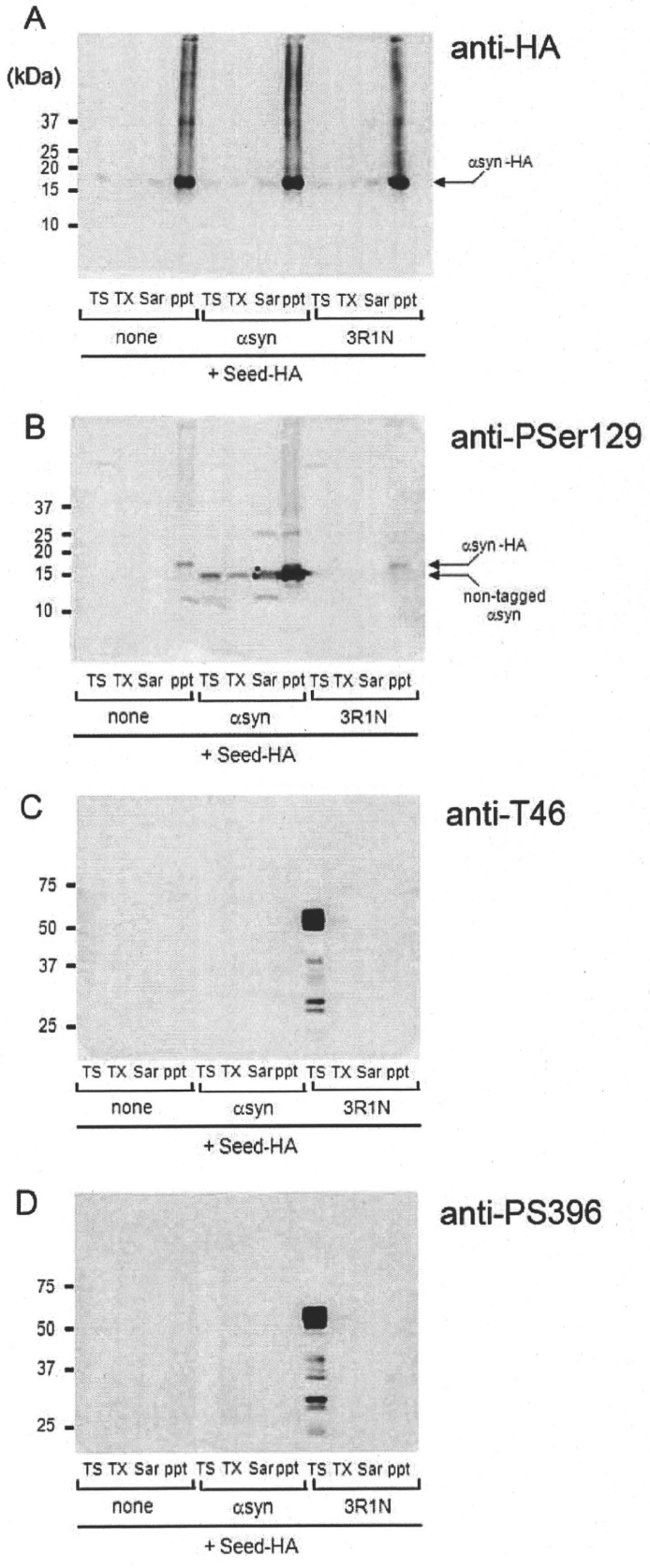

Fig. S4 Nonaka et al

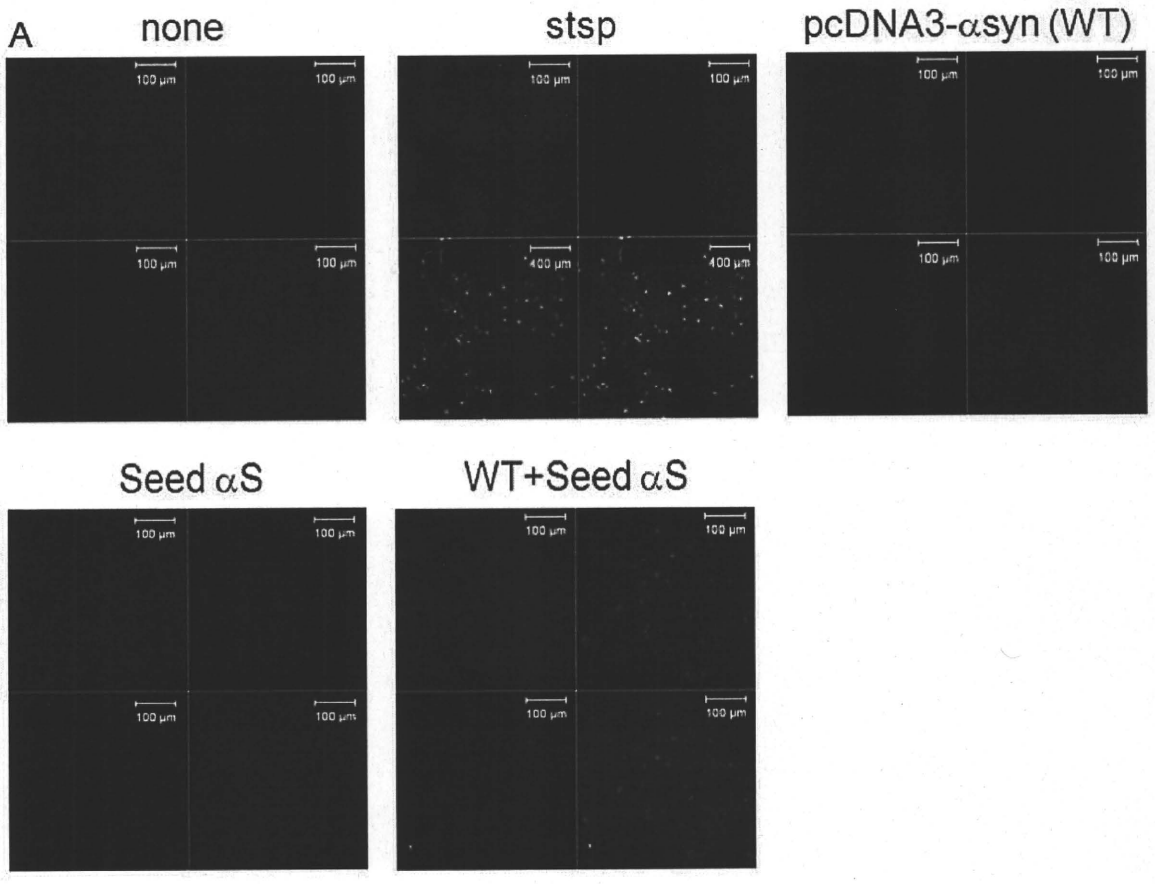

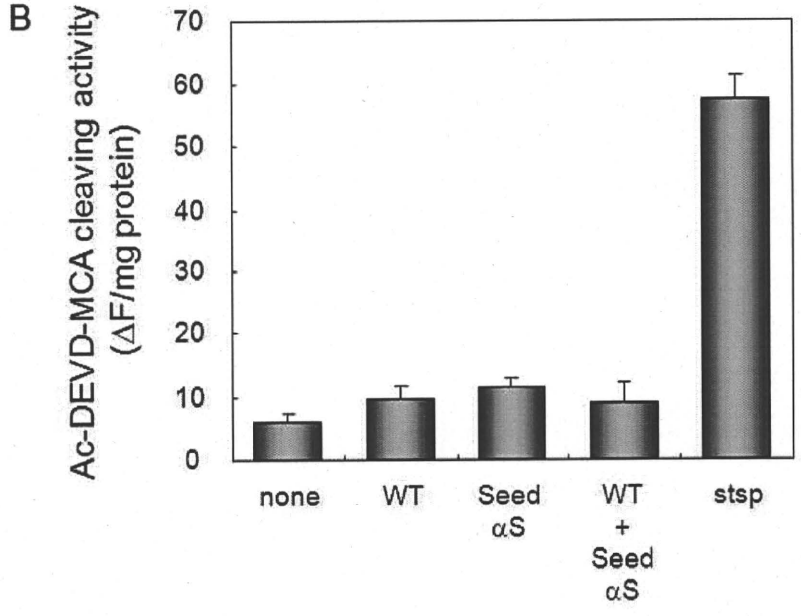

Fig. S5 Nonaka et al

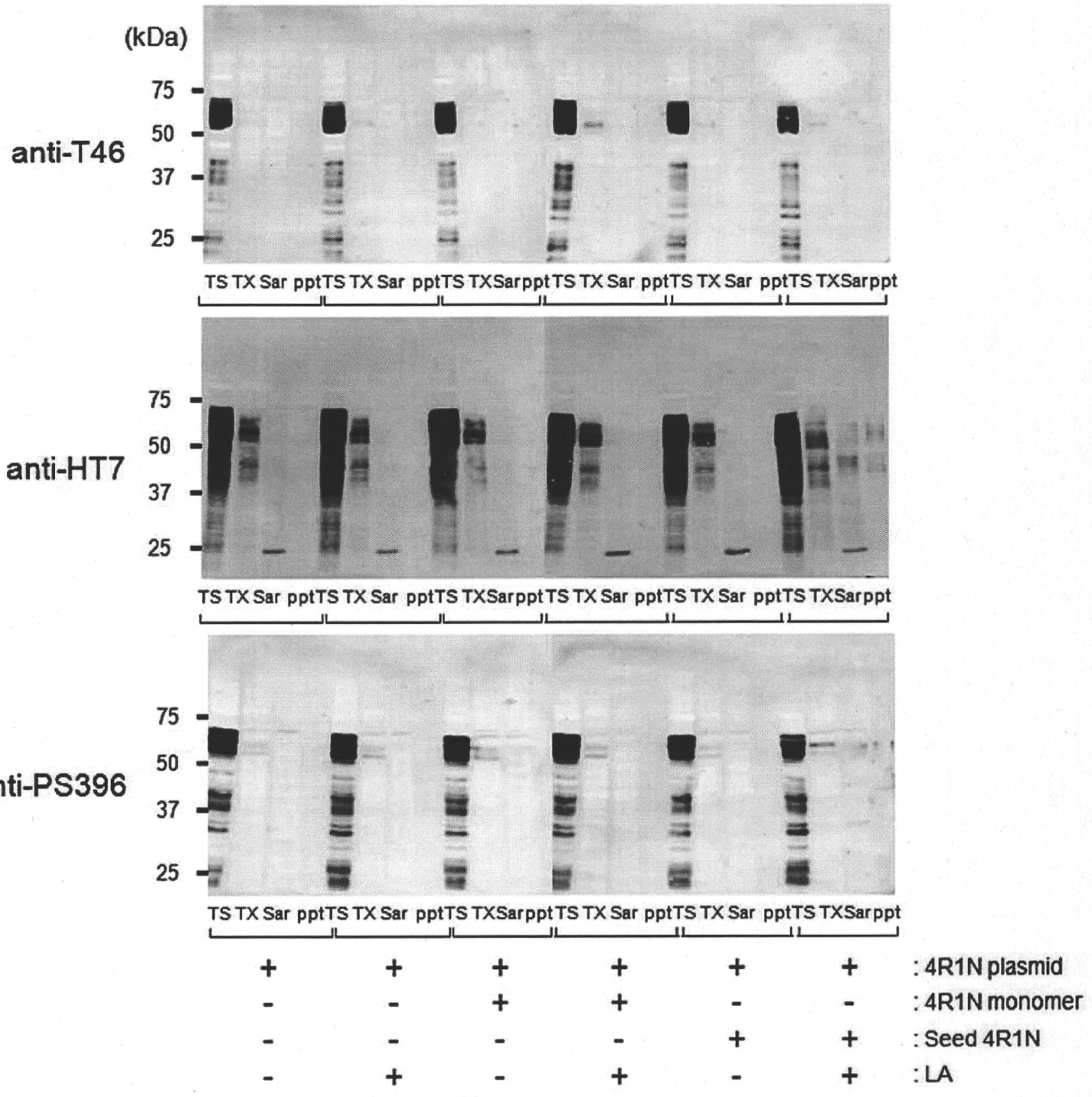

doi:10.1016/j.jmb.2009.10.068 J. Mol. Biol. (2010) 395, 445–456

JMB

Available online at www.sciencedirect.com

ScienceDirect

ELSEVIER

Characterization of Inhibitor-Bound α-Synuclein Dimer: Role of α-Synuclein N-Terminal Region in Dimerization and Inhibitor Binding

Yoshiki Yamaguchi[1,2*†], Masami Masuda[3,4†], Hiroaki Sasakawa[1,5], Takashi Nonaka[3], Shinya Hanashima[2], Shin-ichi Hisanaga[4], Koichi Kato[1,5,6] and Masato Hasegawa[3*]

[1]*Department of Structural Biology and Biomolecular Engineering, Graduate School of Pharmaceutical Sciences, Nagoya City University, 3-1 Tanabe-dori, Mizuho-ku, Nagoya 467-8603, Japan*

[2]*Structural Glycobiology Team, Systems Glycobiology Research Group, Chemical Biology Department, RIKEN, Advanced Science Institute, 2-1 Hirosawa Wako, Saitama 351-0198, Japan*

[3]*Department of Molecular Neurobiology, Tokyo Institute of Psychiatry, 2-1-8 Kamikitazawa, Setagaya-ku, Tokyo 156-8585, Japan*

[4]*Molecular Neuroscience Laboratory, Graduate School of Science, Tokyo Metropolitan University, 1-1 Minami-Osawa, Hachioji-shi, Tokyo 192-0397, Japan*

[5]*Institute for Molecular Science, National Institutes of Natural Sciences, 5-1 Higashiyama, Myodaiji, Okazaki, Aichi 444-8787, Japan*

α-Synuclein is a major component of filamentous inclusions that are histological hallmarks of Parkinson's disease and other α-synucleinopathies. Previous analyses have revealed that several polyphenols inhibit α-synuclein assembly with low micromolar IC_{50} values, and that SDS-stable, noncytotoxic soluble α-synuclein oligomers are formed in their presence. Structural elucidation of inhibitor-bound α-synuclein oligomers is obviously required for the better understanding of the inhibitory mechanism. In order to characterize inhibitor-bound α-synucleins in detail, we have prepared α-synuclein dimers in the presence of polyphenol inhibitors, exifone, gossypetin, and dopamine, and purified the products. Peptide mapping and mass spectrometric analysis revealed that exifone-treated α-synuclein monomer and dimer were oxidized at all four methionine residues of α-synuclein. Immunoblot analysis and redox-cycling staining of endoproteinase Asp-N-digested products showed that the N-terminal region (1–60) is involved in the dimerization and exifone binding of α-synuclein. Ultra-high-field NMR analysis of inhibitor-bound α-synuclein dimers showed that the signals derived from the N-terminal region of α-synuclein exhibited line broadening, confirming that the N-terminal region is involved in inhibitor-induced dimerization. The C-terminal portion still predominantly exhibited the random-coil character observed in monomeric α-synuclein. We propose that the N-terminal region of α-synuclein plays a key role in the formation of α-synuclein assemblies.

*Corresponding authors. Y. Yamaguchi is to be contacted at Structural Glycobiology Team, Systems Glycobiology Research Group, Chemical Biology Department, RIKEN, Advanced Science Institute, 2-1 Hirosawa Wako, Saitama 351-0198, Japan. E-mail addresses: yyoshiki@riken.jp; masato@prit.go.jp.

† Y.Y. and M.M. contributed equally to this work.

Abbreviations used: PD, Parkinson's disease; Exi-monomer, exifone-bound monomer; Exi-dimer, exifone-bound dimer; HSQC, heteronuclear single quantum coherence; NBT, nitroblue tetrazolium; MALDI-TOF, matrix-assisted laser desorption/ionization time-of-flight; MS, mass spectrometry.

0022-2836/$ - see front matter © 2009 Elsevier Ltd. All rights reserved.

[6]*Okazaki Institute for Integrative Bioscience, National Institutes of Natural Sciences, 5-1 Higashiyama, Myodaiji, Okazaki, Aichi 444-8787, Japan*

Received 3 April 2009; received in revised form 26 September 2009; accepted 27 October 2009
Available online
3 November 2009

Edited by S. Radford

Keywords: NMR; α-synuclein; dimer; dopamine; Parkinson's disease

Introduction

Parkinson's disease (PD) and other α-synucleinopathies are progressive neurodegenerative diseases characterized by the selective loss of dopaminergic neurons and deposition of filamentous Lewy bodies, of which α-synuclein is the major component. Formation of amyloid fibrils and/or intermediate oligomers of α-synuclein is a complex process, and small-molecular inhibitors have been used to investigate the pathways involved. Conway *et al.* reported that catechol-containing compounds, including dopamine, inhibited the formation of α-synuclein fibrils, causing the accumulation of α-synuclein protofibrils.[1] It was also reported that α-synuclein fibrillization was inhibited by dopamine analogues, and α-synuclein oligomers were stabilized by these compounds.[2] We have previously reported that several polyphenols inhibited α-synuclein assembly with IC_{50} values in the low micromolar range, and that noncytotoxic, SDS-stable α-synuclein oligomers were formed in the presence of inhibitory compounds.[3]

Analyses of the interactions between small-molecular inhibitory compounds and α-synuclein have been reported by many groups, but the mechanisms involved remain controversial. It was proposed that amyloid fibril formation is inhibited by polyphenol compounds *via* noncovalent aromatic interactions with the amyloidogenic core.[4] A recent report showed that chemical aggregates inhibited amyloid formation of the yeast and mouse prion proteins in a manner characteristic of colloidal inhibition, suggesting a nonspecific mechanism.[5] Mutagenesis and competition studies with specific synthetic peptides suggested α-synuclein residues 125–129 (YEMPS) as an important region for dopamine-induced inhibition of α-synuclein fibrillization, and the inhibition was proposed to be due to conformational alterations of α-synuclein induced by noncovalent interaction with oxidized dopamine.[6] Molecular dynamics simulations suggest that dopamine binds to the YEMPS region, and the bound dopamine is further stabilized by long-range electrostatic interactions with E83 in the NAC region.[7] A recent NMR analysis indicated that a polyphenol compound, epigallocatechin gallate, noncovalently binds to the C-terminal region of α-synuclein (D119, S129, E130, and D135).[8] NMR analysis showed that A53T mutant α-synuclein, which is linked to autosomal dominant forms of PD, has a greater propensity to aggregate in the presence of dopamine, compared to wild-type α-synuclein.[9] Meanwhile, NMR characterization of the interaction between α-synuclein and various small molecules indicated that residues 3–18 and 38–51 act as noncovalent binding sites for inhibitory compounds.[10]

Covalent attachment of inhibitors to α-synuclein, on the other hand, has been proposed by several groups. Conway *et al.* suggested that 5–10% of dopamine was covalently incorporated into α-synuclein by radical coupling (dopamine-derived orthoquinone to Tyr) and/or nucleophilic attack (e.g., Lys forming a Schiff base with the orthoquinene).[1] Mass spectrometry (MS) and NMR characterization suggested that the oxidation product (quinones) of a dopamine analogue was covalently linked to the amino groups of the α-synuclein chain, thereby generating α-synuclein–quinone adducts.[2] Thus, the binding mode and binding site(s) of small-molecular inhibitors remain controversial.

The conformation of inhibitor-induced α-synuclein oligomers is also a matter of debate. Norris *et al.* reported that spherical oligomers of dopamine-modified α-synuclein take a predominantly random-coil structure with some β-pleated sheets on the basis of CD and Fourier-transform infrared spectroscopy studies.[6] Another group demonstrated that in the presence of small inhibitory molecules, α-synuclein is still dominated by random-coil character.[10] Ehrnhoefer *et al.* proposed that epigallocatechin prevented the conversion of monomeric α-synuclein into toxic on-pathway aggregation intermediates and resulted in the formation of unstructured, nontoxic α-synuclein oligomers that they considered to be off-pathway.[8] On the other hand, it has recently been reported that a flavonoid, baicalein, stabilized β-sheet-enriched oligomers based on CD and Fourier-transform infrared spectroscopy analysis.[11] The baicalein-stabilized oligomers were characterized as quite compact globular species based on small-angle X-ray scattering data and atomic force microscopy.

Masuda *et al.* isolated α-synuclein dimers formed in the presence of inhibitory compounds,[3] and the isolated soluble dimers were recently characterized using a panel of epitope-specific α-synuclein antibodies.[12] The reactivities of the antibodies indicated that the conformations of polyphenol-bound α-synuclein dimers differ from those of unbound monomers, but resemble those of amyloid fibrils, suggesting that inhibitor-bound molecular species are on-pathway intermediates.

This situation prompted us to carry out a comprehensive analysis of inhibitor-treated α-synucleins by means of NMR spectroscopy in conjunction with other biochemical methods, such as peptide mapping, immunoblotting, and redox-cycling staining. We have previously analyzed the antibody binding and site-specific phosphorylation of α-synuclein using ultra-high-field NMR spectroscopy.[13] For the structural characterization, we prepared and purified a ^{15}N-labeled α-synuclein dimer in the presence of polyphenol inhibitors on a milligram scale and analyzed it by ultra-high-field NMR spectroscopy recorded at a proton observation frequency of 920 MHz.

Results and Discussion

Isolation and characterization of inhibitor-bound α-synuclein dimer and monomer

SDS-stable, noncytotoxic α-synuclein oligomers were detected in the soluble fraction in the presence of inhibitory compounds such as polyphenols.[3] For detailed characterization of inhibitor-induced α-synuclein oligomers, we attempted to prepare exifone-, gossypetin-, and dopamine-induced α-synuclein dimer and monomer (for inhibitor structures, see Fig. 1) and to separate them by gel-filtration chromatography as described.[12] Fig. 2a shows the HPLC patterns of control and exifone-treated α-synucleins. The HPLC fractions of exifone-treated α-synuclein were analyzed by SDS-PAGE and Western blotting (Fig. 2b). The data indicate that the exifone-treated α-synuclein dimer (Exi-dimer) was successfully purified by gel-filtration chromatography. The homogeneity of inhibitor-induced monomer and dimer was also checked by diffusion NMR experiments (data not shown). α-Synuclein monomer and dimer treated with exifone, as well as control monomer (without inhibitor), were subjected to matrix-assisted laser desorption/ionization time-of-flight (MALDI-TOF) MS measurements (Fig. 2c). α-Synuclein monomer (control) showed a major signal at 14,460 Da, which matched the predicted mass (14,460 Da). On the other hand, exifone-treated monomer (Exi-monomer) gave a major signal at 14,524 Da, which corresponded to that of α-synuclein plus 64 Da. Exifone-bound α-synuclein (molecular mass of exifone, 278.2 Da) was not detected, presumably because exifone binding was noncovalent. The MS spectrum of Exi-dimer showed a broad peak at around 30 kDa and 15 kDa, and we could not obtain an accurate molecular mass. The peak at 15 kDa might be the doubly charged ion of the Exi-dimer and/or the monomer released from the Exi-dimer in the ionization process. To estimate the ratio of exifone bound to α-synuclein dimer and monomer, absorption of exifone at 385 nm was measured for Exi-dimer and Exi-monomer. The results indicate that Exi-dimer contains around 3

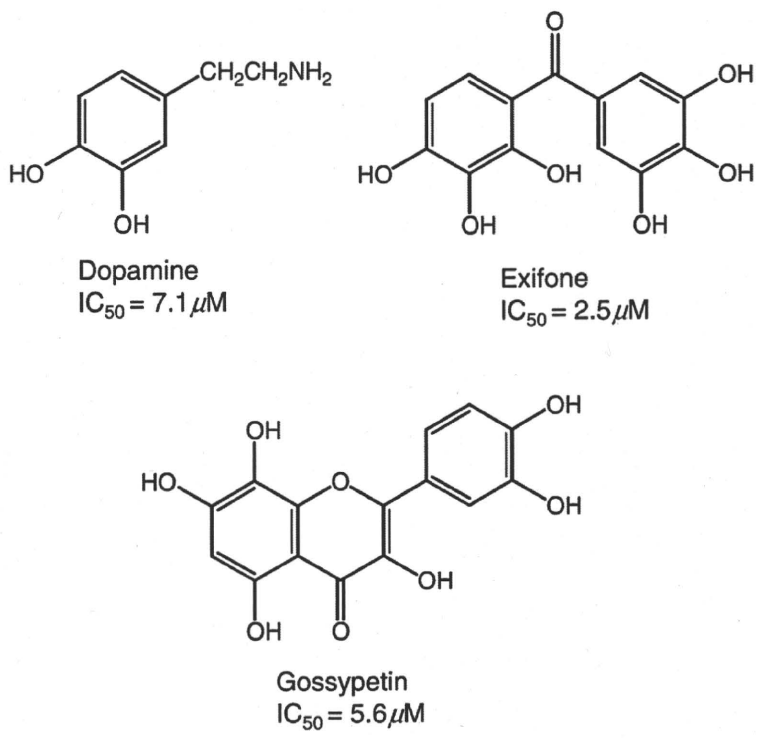

Fig. 1. Chemical structures of dopamine, exifone, and gossypetin with their IC_{50} values for inhibition of α-synuclein filament assembly.[3]

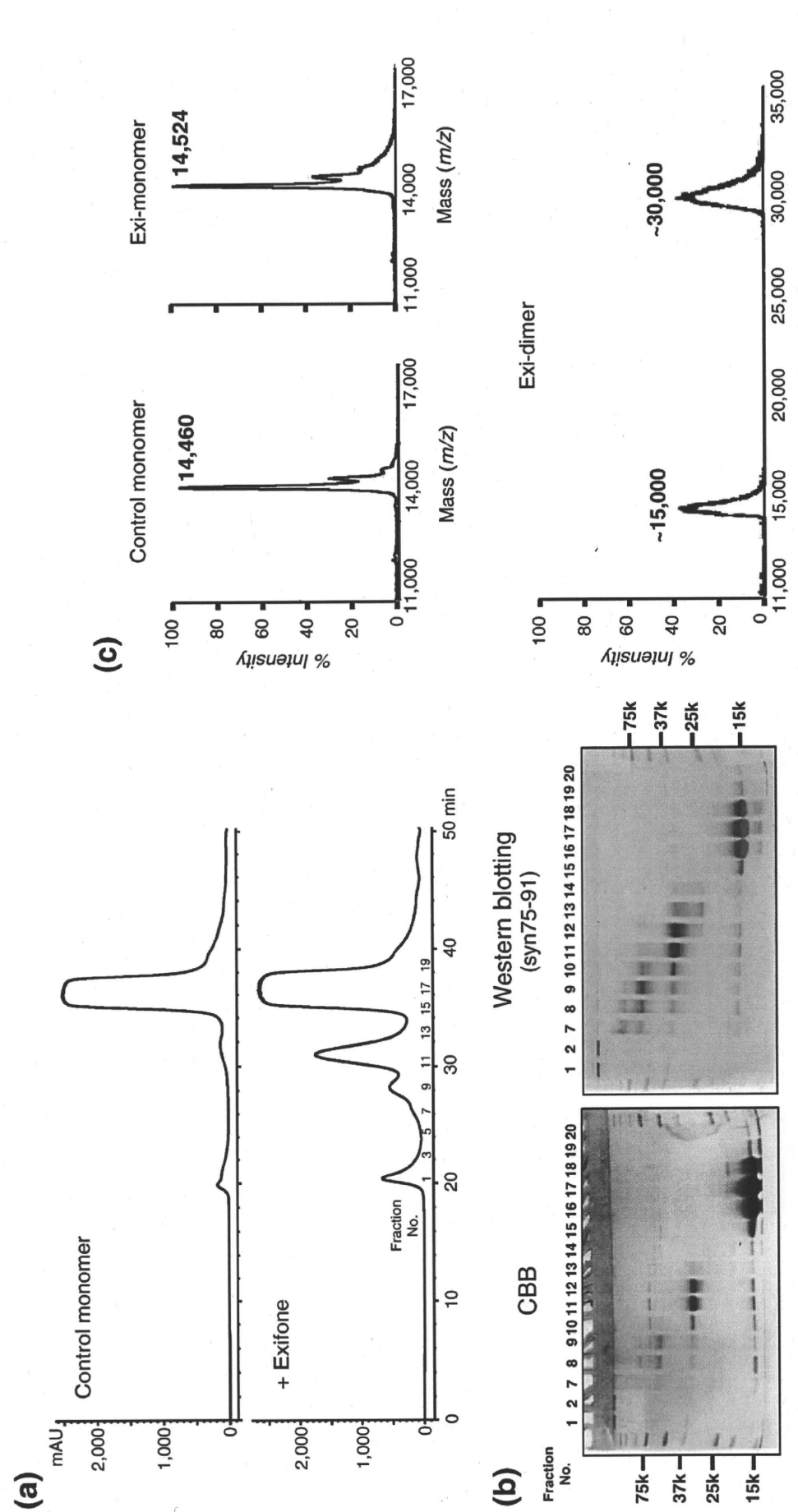

Fig. 2. Isolation and characterization of exifone-bound α-synucleins. (a) Separation of exifone-treated α-synuclein monomer and dimer by gel-filtration chromatography (detection: absorbance at 214 nm). (b) SDS-PAGE of fractions separated by gel-filtration chromatography (Coomassie brilliant blue staining and Western blotting). Pooled fractions 11–12 and 16–18 were used as Exi-dimer and Exi-monomer, respectively. (c) Partial MALDI-TOF MS spectra of α-synuclein monomer (control), Exi-monomer, and Exi-dimer.

molecules of exifone per α-synuclein monomer, while Exi-monomer contains one exifone molecule per α-synuclein chain (Supplementary Fig. S1).

For the identification of the modification (corresponding to a molecular mass of 64 Da) found in the Exi-monomer, α-synuclein was incubated with various concentrations of exifone (0, 0.2, 0.5, 1, and 2 mM) and the resulting samples were analyzed by MS (Supplementary Fig. S2). The molecular mass of α-synuclein increased in an exifone concentration-dependent manner and reached 14,528 Da (Supplementary Fig. S2a and b). A similar increase in molecular mass was reported in the presence of H_2O_2, which oxidized methionine residues to methionine sulfoxide.[14] Methionine oxidation is known to increase mass by 16 Da. α-Synuclein has four methionine residues, Met1, Met5, Met116, and Met127, and thus the oxidation of all the methionine residues would result in an increase in mass of 64 Da (Supplementary Fig. S3c). Indeed, α-synuclein incubated with various concentrations of H_2O_2 showed a concentration-dependent increase in molecular mass of up to 14,533 Da (Supplementary Fig. S3a and b), similar to that seen in the case of exifone. These results strongly suggest that all the methionine residues of Exi-monomer were oxidized to methionine sulfoxide.

Peptide mapping of inhibitor-induced α-synuclein dimer and monomer

In order to confirm the oxidation of methionine, control α-synuclein, Exi-monomer, Exi-dimer, and H_2O_2-treated α-synuclein monomer were digested with trypsin, and the resulting peptide mixtures were analyzed by reverse-phase HPLC (Fig. 3a). The elution patterns of peptides derived from Exi-monomer and Exi-dimer exhibited different profiles compared with that of control α-synuclein. Peaks 5 and 10 in the map of control α-synuclein were absent in the maps of Exi-monomer and Exi-dimer. Instead, peaks 11–18 newly appeared in the maps of Exi-monomer and Exi-dimer. The patterns of Exi-monomer and Exi-dimer were similar to those of α-synuclein oxidized with H_2O_2. All the peaks were analyzed by MS and the results are summarized in Fig. 3b. Peaks 5 and 10 were identified as Met1–Lys6 (containing two methionines, Met1 and Met5) and Asn103–Ala140 (containing Met116 and Met127), respectively. In the case of Exi-monomer or Exi-dimer, peaks 11, 15, and 19 were identified as Met1–Lys6 including two oxidized methionines. Peaks 12, 16, and 20 were identified as Asn103–Ala140 including oxidized Met116 and Met127. Peaks 13, 14, 16, and 17 were derived from Asn103–Ala140 oxidized at either Met116 or Met127. Similar results were obtained for dopamine-bound dimer and monomer (data not shown). These results clearly indicate that the inhibitors exifone and dopamine have the ability to oxidize methionine residues on α-synuclein. It is established that α-synuclein assembly was inhibited by exifone at low micromolar range (IC_{50}=2.5 μM),[3] and methionine sulfoxide could not be detected at a low concentration of exifone (data not shown). These findings suggest that the stabilization of intermediate oligomers by small molecules is responsible for the inhibition of filament formation, and oxidation of methionine does not seem to play a major role in inhibition.

No covalent inhibitor–peptide adducts or cross-linked peptides were detected in the peptide mapping experiments, indicating that the inhibitors bind noncovalently to α-synuclein and that α-synuclein dimer is formed in a noncovalent fashion. These observations are consistent with the results of MALDI MS analysis of Exi-monomer, which showed no inhibitor adducts (Fig. 2c). Our extensive liquid chromatography–electrospray ionization MS analysis also did not show the covalent inhibitor adducts or α-synuclein dimer (data not shown). Further, more detailed biochemical studies to investigate the modes of inhibitor binding and dimerization are currently in progress.

Characterization of exifone-binding regions in α-synuclein

Exifone is an antioxidant and thus can be detected by redox-cycling staining, which is a well-established method for detecting quinoproteins.[15] As expected, Exi-dimer and Exi-monomer were stained as purple bands by redox-cycling staining due to nitroblue tetrazolium (NBT) reduction to formazan (Fig. 4a), while untreated control α-synuclein showed no staining. This result shows that redox-cycling staining is useful for examining the exifone-binding regions in α-synuclein. In order to determine the binding region of exifone and the regions involved in the dimerization, Exi-dimer was digested with endoproteinase Asp-N and the resulting peptides were detected with silver or redox-cycling staining. Asp-N digestion of Exi-dimer gave two major fragments, corresponding to molecular masses of 20 kDa (no. 1) and 16 kDa (no. 2), on SDS-PAGE after silver staining (Fig. 4b). These two bands were positive for redox-cycling staining. Since α-synuclein monomer migrates at 15 kDa, these fragments represent dimeric peptides stabilized by exifone. α-Synuclein has six aspartic acid residues (Asp2, Asp98, Asp115, Asp119, Asp121, and Asp135). Immunoblot analysis with a panel of site-specific anti-α-synuclein antibodies (Fig. 5) suggested that the 20-kDa fragment contains the dimerized N-terminal fragment Met1–Met97 of α-synuclein (cleaved at the N-terminus of Asp98). The 16-kDa fragment was also labeled with antibodies to the N-terminal and central portions of α-synuclein (residues 1–50). It has been reported that Asp-N cleaves peptide bonds N-terminal to glutamate as well as aspartate residues.[16,17] Glu57 and/or Glu61 are found in the middle of α-synuclein and are candidate Asp-N cleavage sites to produce the 16-kDa fragment. The reactivity of anti-α-synuclein antibodies and the relaxed specificity of Asp-N indicate that the 16-kDa fragment corresponds to a dimer composed of Met1–Ala56/Lys60. These results suggest that the N-

terminal region (1–60) of α-synuclein is involved in the dimerization and exifone binding. This is in contrast with a previous report by Norris *et al.*, in which they suggested that dopamine inhibited the aggregation of α-synuclein by binding to the C-terminal residues 125–129 (i.e., YEMPS) and stabilizing the soluble oligomers.[6] The discrepancy might be due to the fact that they analyzed the dopamine-binding sites by using deletion mutants lacking the C-terminal regions and did not use full-length α-synucleins.

High-resolution NMR spectra of inhibitor-bound α-synuclein monomer and dimer

In order to characterize the behavior of α-synuclein monomer and dimer formed in the presence of polyphenolic compounds, we conducted a structural analysis of inhibitor-bound α-synuclein monomer and dimer using ultra-high-field NMR spectroscopy. NMR signals of backbone amides constitute excellent probes to provide maps of the interacting sites and to examine the effects of modifications.[13] Fig. 6a and b shows the ^{1}H–^{15}N heteronuclear single quantum coherence (HSQC) spectra of uniformly ^{15}N-labeled Exi-monomer and Exi-dimer, as well as control monomer, recorded at a proton observation frequency of 920 MHz. The amide resonances of Exi-monomer and Exi-dimer were assigned by comparing the NMR spectral data with those of control α-synuclein monomer. Little chemical shift difference was detected between Exi-monomer and control monomer for most observed peaks, except for the signals corresponding

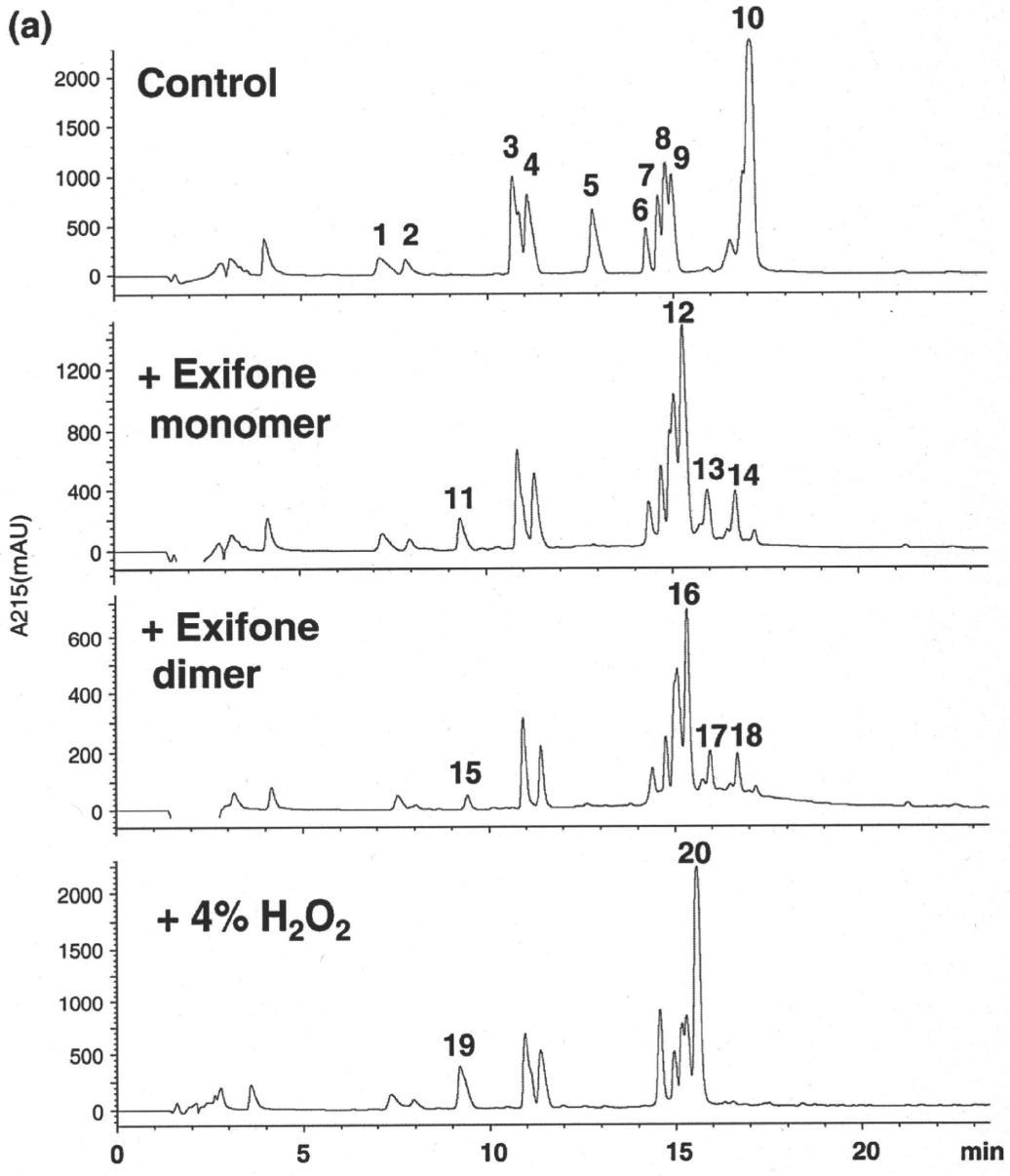

Fig. 3. Tryptic peptide mapping and MS analysis of α-synucleins. (a) Reverse-phase HPLC patterns of monomeric α-synuclein (control), Exi-monomer, Exi-dimer, and H_2O_2-treated α-synuclein monomer. (b) Observed masses and peak assignments of the peptides separated on a reverse-phase column. Oxidation of methionine residues was observed in Exi-monomer and Exi-dimer, as well as H_2O_2-treated α-synuclein monomer.